AUTOMATED UPDATING OF BUILDING DATA BASES FROM DIGITAL SURFACE MODELS AND MULTI-SPECTRAL IMAGES: POTENTIAL AND LIMITATIONS

Franz Rottensteiner

Cooperative Research Centre for Spatial Information, Dept. of Geomatics, University of Melbourne, 723 Swanston Street, Melbourne VIC 3010, Australia - franzr@unimelb.edu.au

Commission III, WG III/4

KEY WORDS: Change Detection, Digital Surface Models, Data Fusion

ABSTRACT:

A method for automatic updating of building data bases from Digital Surface Models (DSM) and a normalised difference vegetation index is evaluated. The DSM can be generated from Airborne Laserscanner (ALS) data or by image matching techniques. Buildings are detected automatically from the input data. The building detection results are compared to an existing building data base, and changes between the existing data base and the new data set are determined. Buildings and building parts are classified as being *confirmed*, *changed*, *new*, or *demolished*. Change detection considers the fact that the original data and the building detection results can have a different topology and that small differences between the data from the two epochs might be caused by generalisation errors, by a misalignment of the data, or by insufficient sensor resolution. The performance of the algorithm is analysed using DSMs generated both from ALS data and by image matching. The evaluation shows the different properties of these data for building change detection and also some of the limitations of the method. If the accuracy requirements for the building outlines are not very high, the automatic updating process can be automated, provided that high-quality DSMs are used. In a semi-automatic environment the amount of human interaction for updating building data bases can be reduced by 40%-60%.

1. INTRODUCTION

In many industrial countries there exist 2D topographic data bases with a building layer. Keeping such a data base up-to-date has been estimated to require up to 40% of the costs necessary to generate it from scratch (Champion, 2007). To reduce these costs it is desirable to automate this process. Using high-resolution aerial imagery and / or airborne laser scanner (ALS) data, it should be feasible to detect changes of urban development automatically (Matikainen et al., 2004, Champion, 2007). If the accuracy requirements are not very high, human intervention can be restricted to a check of the changed building outlines and a manual digitisation of incorrect or inaccurate results. Even if the accuracy requirements are high (e.g. for updating the cadastre), the manual effort required for map updating can be reduced significantly by embedding automated change detection into a semi-automatic system. In such a system, the automated module focuses the human operator's attention by highlighting areas of change. Whereas the new building outlines are still digitised manually, the amount of human interaction is reduced because buildings found to be unchanged by the automated process need not be inspected at all and because potential new buildings are already highlighted.

There are two general strategies for change detection: It can be based either on a comparison of sensor data for two different epochs or on a comparison of an existing data base to more recently collected sensor data (Vosselman et al., 2004). If 3D data are available for the acquisition time of the original data base, changes in buildings will result in height differences between the original data and a more recently acquired DSM, which can be used for change detection. Vögtle and Steinle (2004) presented such an algorithm. Based on an evaluation of the overlap ratios between buildings in the old and the new data sets, buildings are initially classified as *new*, *demolished*, or *other*. The height changes between the original DSM and the more recently acquired data are evaluated to further classify *other* buildings as *not-altered*, *added-on*, or *reduced*. If no 3D data are available for the acquisition time of the original data, it is a common strategy for change detection to first detect buildings in the new data and then compare the building footprints thus derived to the original data base. Vosselman et al. (2004) present a method for comparing an existing map with the results of a building detection technique using ALS data. They give a list of errors that might result in differences between the existing map and the newly extracted buildings and show how to compensate for the errors caused by generalisation and false alignment. Matikainen et al. (2004) detect buildings in ALS data and aerial images and compare the results to an existing building data base. Buildings in the existing data base are classified as *detected*, *partly detected*, and *not detected*, whereas buildings in the new data set are classified as *new*, *enlarged,* or *old*. A joint visualisation of these classification results is presented on a per-pixel basis, but no further object-based analysis is carried out. Champion (2007) uses a DSM generated by image matching to verify the buildings of an existing data base. The original building outlines are compared to step edges extracted from the DSM. A similarity measure evaluating the percentage of the length of the building outlines having a match in the set of step edges is used to classify a building as *validated*, *modified*, or *destroyed*. *New* buildings are detected using the DSM and a tree layer derived from multi-spectral images and the DSM.

In (Rottensteiner, 2007), a method for building change detection from a DSM and a normalised difference vegetation index (NDVI) derived from a multi-spectral image was presented. It is based on a comparison of the results of an algorithm for automatic building detection (Rottensteiner et al., 2007) to the existing map, taking into account that deviations between the two data sets might be due to different degrees of generalisation and to small registration errors. This method will

be presented in a revised form in Section 2. The main goal of this paper is a thorough evaluation of this method. In (Rottensteiner, 2007), first results achieved for two different data sets were presented, and a pixel-based evaluation of the updated building data base showed that DSM errors had a significant impact on the classification accuracy. In Section 3, a more thorough evaluation will be carried out using the same data sets. Confusion matrices of the different change classes will be presented, and completeness and correctness will be assessed for each of these classes. The separability of these classes will be discussed, and the effectiveness of the method in reducing human intervention in a semi-automatic environment as described above will be assessed. The results achieved for DSMs from ALS and image matching will also be compared. Conclusions will be drawn in Section 4.

2. BUILDING CHANGE DETECTION

Building change detection requires a DSM generated by image matching or from ALS data. Optionally, a geocoded NDVI image and a model of the height differences between the first and last pulses of ALS data can be used, too. These input data, along with a Digital Terrain Model (DTM) generated from the DSM by hierarchic morphologic filtering, are used for building detection based on the theory of Dempster-Shafer for data fusion (Rottensteiner et al., 2007). The existing building data base can also be considered in this process. The results of building detection are compared to an existing building data base, and changes between the existing data base and the new data set are determined by a comparison of two label images: the "existing label image" L^e and the "new label image" L^n. Change detection starts with a topological clarification in order to achieve topological consistency between the two label images. This is followed by the actual classification of changes. It is the goal of change detection to (1) classify the buildings in the existing data base as *confirmed*, *changed*, or *demolished*, (2) detect *new* buildings, (3) show *demolished* and *new building parts* for the *changed* buildings, and (4) determine the outlines of the *changed* and the *new* buildings. The individual stages of change detection will be described in the subsequent sections.

2.1 Building Detection

Building detection starts with a Dempster-Shafer fusion process carried out for each pixel of the DSM to achieve a classification of the input data into one of four classes: buildings, trees, grass land, and bare soil. A heuristic model for the distribution of the evidence from each input data set to the four classes is applied. Initial building regions are determined as connected components of building pixels. A second Dempster-Shafer fusion process eliminates regions still corresponding to trees. The new label image L^n is one of the results of the building detection algorithm (Rottensteiner et al., 2007).

For building change detection the existing label image L^e can be used as a further input data set in the first Dempster-Shafer fusion process. Usually the amount of change will be limited, so that the original data base gives an indication where buildings are to be expected. This can be modelled by the probability P_C that the status of a pixel has changed. If a pixel is inside the building in L^e, the probability of the pixel still being inside a building at the later epoch is $(1 - P_C)$, whereas the probability that it is no longer inside a building is P_C. If a pixel is not inside a building in L^e, the probability of the pixel being inside a building at the later epoch is P_C, whereas the probability that it is still not a building is $(1 - P_C)$. This can be used as a model for the assignment of probability masses to the four object classes. Thus, the original data base introduces a bias for no changes to have occurred into the classification process. P_C is chosen by the user, typically between 20 % and 40 %.

2.2 Topological Clarification

In order to achieve topological consistency between the existing label image L^e and the new label image L^n, correspondences between labels from the two data sets must be found. For each co-occurrence of two labels $l^e \in L^e$ and $l^n \in L^n$, the overlap ratios $p_{ne} = n_{n \cap e} / n_n$ and $p_{en} = n_{n \cap e} / n_e$ are computed, where $n_{n \cap e}$ is the number of pixels assigned to l^n in L^n and to l^e in L^e, n_n is the total number of pixels assigned to l^n, and n_e is the total number of pixels assigned to l^e. Correspondences with both p_{ne} and p_{en} smaller than a threshold t_m (e.g. 10 %) are eliminated. If the topology of the two data sets was identical except for *new* or *demolished* buildings, each label would have exactly zero or one corresponding label in the other data set. As this is usually not the case, each label can have zero, one, or more correspondences. If a label in L^e has M corresponding labels in L^n, the original building is split into M parts. This can reflect the actual demolition of a building part or not, because the building detection algorithm tends to split buildings at height discontinuities. If a label in L^n has N corresponding labels in L^e, N existing buildings are merged. This occurs with terraced houses having identical roof heights. If a set of M labels $l_i^e \in L^e$ corresponds to a set of N labels $l_j^n \in L^n$, buildings are both split and merged, and there are ambiguities with respect to the correct correspondences of some of the new labels.

2.2.1 Clarification of the ambiguous cases: This is achieved by modifying the new label image. Any label l^n that corresponds to more than one label in L^e and / or has a significant overlap with the background is split into two or more labels. First, new buildings are identified. A binary image of *new* building pixels (i.e., building pixels in the new label image corresponding to the background in the existing label image) is generated. Morphological opening is used to remove noise at the building outlines. If there remain *new* building pixels in the filtered image, new labels corresponding to new building parts are detected by a connected component analysis. A label image L^c combining the existing labels L^e and these new labels is created. Each label in L^n corresponding to more than one label in L^c is split so that each of the new labels corresponds to exactly one label of L^c. To compensate for smoothing effects of the morphological filter at the fringes of new building parts, the Voronoi diagram of L^c is used to assign pixels to one of the new labels.

2.2.2 Clarification of the merged cases: Labels can be merged because the buildings are close to each other or because a new building has been constructed between them. In a similar way as described above, new building labels are detected. The merged label in L^n is split into several new labels, each corresponding to a new building or to exactly one label in L^e.

2.2.3 Clarification of the split cases: This clarification process starts with growing the new labels by morphologic closing. If two labels are found to be neighbours in the closed label image, the splitting is supposed not to be caused by a real change, and the two labels are merged in L^n. Otherwise, the separation is assumed to be the result of the demolition of a building part, and the original labels are maintained.

2.3 Classification of Changes

As a result of topological clarification, an improved version L^n_{imp} of the new building label image L^n is obtained. Each of the labels in L^n_{imp} corresponds to zero or to one label in L^e. Each of the labels of L^e corresponds to zero, one, or N labels of L^n_{imp}. Again, overlap ratios are computed for each co-occurrence of two labels $l^e \in L^e$ and $l^n \in L^n_{imp}$, and marginal correspondences are eliminated. A building is classified as *new* if its label $l^n \in L^n_{imp}$ does not have any correspondence in L^e. An existing building is classified as *demolished* if its label $l^e \in L^e$ does not have any correspondence in L^n_{imp}. For all remaining labels $l^e \in L^e$, a binary image of *demolished* pixels (pixels assigned to l^e in L^e, but not to any of its correspondences in L^n_{imp}) and a binary image of *new* pixels (pixels assigned to any of the correspondences of l^e in L^n_{imp}, but not to l^e in L^e) are created. If neither *demolished* nor *new* pixels remain after a morphological opening of these binary images, the building is classified as *confirmed*; otherwise, it is classified as *changed*. For *changed* buildings, connected components in the binary images of *demolished* and *new* pixels are considered to correspond to *demolished building parts* and *new building parts*. For a *changed* building l^e having multiple correspondences in L^n_{imp}, the area corresponding to the label in L^n_{imp} having the largest overlap with l^e is classified as *changed*. All the other labels corresponding to that building could also be classified as *changed* from the point of view of the existing data base. However, in the updated data base, these labels will correspond to new entities, so that they could also be classified as *new*. Thus, the new class *split off* is introduced for these "new" buildings corresponding to a part of an existing one (Fig. 1).

Figure 1. Classification of changes for multiple overlap cases. Left top: original label image. Left bottom: results of topological clarification. Right: change map.

After the classification, two images representing the change detection results are generated: (1) a *change map* using different colours for *new*, *demolished*, *confirmed*, and *split off* buildings as well as for *confirmed*, *new*, and *demolished parts* of *changed* buildings, and (2) a label image representing the new state. For generating the label image representing the new state, there are two options. The first option is to use the improved version of the new label image. If the original map is more accurate, the original outlines can be used for *confirmed* buildings, whereas the new outlines of *changed* and *split off* buildings can be a combination of the original outlines for the unchanged building parts and the outlines of the *new building parts*.

3. EXPERIMENTS

3.1 The Test Data Sets

The first data set used for evaluation was captured over Fairfield (NSW). It consisted of ALS points with a spacing of 1.2 m. The first and the last laser pulses as well as the intensity of the returned signal were recorded. A colour stereo pair and a digital orthophoto with a ground resolution of 0.15 m were also available. From the red band of the orthophoto and the intensity of the ALS signal, a "pseudo-NDVI" image was generated. DSMs of a grid width $\Delta = 1$ m were derived for both the first and the last pulse data. The outlines of the buildings were determined by photogrammetric plotting with a planimetric accuracy of 0.2 m. In order to simulate actual changes, the existing data base was generated from these outlines by adding and removing buildings or building parts. The size of the test area was 500 x 400 m^2. The second data set, covering an area of about 1100 x 1100 m^2 in Toulouse (France), was provided by EuroSDR (EuroSDR, 2007). It consisted of a DSM generated by image matching, an RGB and an infrared orthophoto, and an existing building data base. Both the DSM and the orthophotos had a resolution of $\Delta = 0.501$ m. The DSM was very noisy, especially in the shadow regions. The numerical resolution of the DSM heights was identical to Δ, so that the only height values occurring were full multiples of Δ. Reference data were generated by digitizing the building outlines in the digital orthophoto with a planimetric accuracy of about 1.0 m.

3.2 Results and Discussion

In Fairfield, the algorithm for building detection described in Section 2.1 was applied to the DSMs generated from ALS data, the surface roughness parameters and the pseudo-NDVI. In Toulouse, the DSM and an NDVI generated from the orthophotos were used. Surface roughness was not considered. In both cases, the parameters of the algorithm were tuned in the way described in (Rottensteiner et al., 2007). Furthermore, the existing data base was considered in both cases, setting the probability of a change to $P_C = 35$ %. In the change detection process, the size of the structural element used for morphologic filtering (cf. Sections 2.2 and 2.3) was set to 3 m. Thus, changes having a smaller linear extent smaller than 3 m could not be detected. This compensates for small misalignments between the existing data base and the new data and for errors of building detection at the building outlines (Rottensteiner et al., 2007). The change detection algorithm was also used to compare the original data base to the reference. The resulting change maps, including the reference, are presented in Figures 2 and 3 for Fairfield and Toulouse, respectively. In Fairfield, the change map was generated using a grid width of 0.5 m; in Toulouse it was identical to the DSM grid width (0.501 m).

In Fairfield, changes affecting the main buildings are detected correctly, even though it can be seen that in some cases, *new* building parts are classified as *new* buildings and vice versa. The separation of these classes is difficult. In case of doubt, the change detection algorithm assumes a new building. The few incorrect *new* building parts are the result of an over-estimation of the building extents. All *demolished* buildings and building parts were detected. All except two *demolished* building parts are correct. However, with *demolished* buildings, the trend observed in (Rottensteiner et al., 2007) is confirmed: For small structures, the results of building detection become uncertain. Thus, the small buildings classified as *demolished* in the back yards, mostly garden sheds and garages, were not really demolished, but they were actually too small to be detected.

The results achieved in Toulouse are not as good as those achieved in Fairfield due to the poor quality of the DSM. Again, it can be observed that small buildings are not detected in the new data set. Some changes are detected correctly, e.g. the *new* and *demolished* buildings in the south-west of the scene. However, there are two large areas of false positive detections: the area in the northeast corner of the scene merges a correctly detected new building with a parking lot, and the area in the east is actually a sports field. In both cases the DSM

had height variations larger than 3 m in essentially horizontal areas. The obvious over-estimation of the large building complex in the western part of the scene is caused by the uncertainty of the DSM in the shadow areas. Other problems were related to trees partly overhanging buildings and to the general lack of ground points in the forested areas.

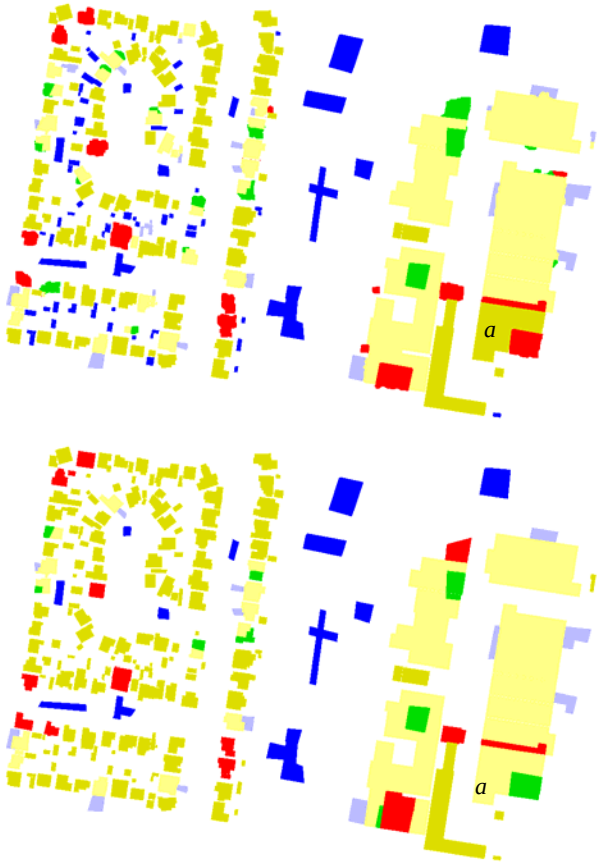

Figure 2. Change maps for Fairfield. Top: Results of automatic change detection. Bottom: Reference. Ochre/yellow: *confirmed* buildings / *building parts*. Blue/light grey: *demolished* buildings / *building parts*. Red/green: *new* buildings / *building parts*.

3.3 Evaluation of the Results

In order to evaluate the results, the change maps derived by the automatic process were compared to the reference change map. Confusion matrices and the derived quality metrics *completeness* and *correctness* (Rottensteiner et al., 2007) were determined on a per-pixel basis. For the Fairfield data set, these metrics were also derived on a per-building basis to assess the effectiveness of the automated process in reducing the amount of human intervention.

3.3.1 Fairfield: Table 1 shows the per-pixel confusion matrix for the change detection results obtained for the Fairfield data set. The completeness and correctness of the results on a per-pixel basis are shown in Table 2. At a first glance, the quality metrics in Table 2 do not look very good. The only class with both completeness and correctness larger than 90% is *changed*. The class having both the worst completeness and the worst correctness is *new building part*, closely followed by *new* building. Table 1 reveals that this is caused by the fact the separation between these classes is very uncertain. The confusion matrix also shows that another major source of error

Figure 3. Change maps for Toulouse. Top: Results of automatic change detection. Bottom: Reference. Ochre/yellow: *confirmed* buildings / *building parts*. Blue/light grey: *demolished* buildings / *building parts*. Red/green: *new* buildings / *building parts*. Pink: *split-off* buildings.

is a misclassification of *confirmed* pixels as *changed*, and vice versa. These problems are connected. If a new building structure is found and if it is classified as a *new building part*, the existing building will be classified as *changed*; if the new structure is classified as a *new building*, the existing building is not affected and might be classified as *confirmed*. This becomes obvious for building *a* in Fig. 2. Whether a new building structure is a new building or an addition to an existing building cannot really be decided by the automated process, because this might actually be determined by circumstances such as property boundaries that are not reflected in the sensor data at all.

It can be argued that on a per-pixel level, the separation between the classes *confirmed* and *changed* is not very

meaningful. After all, both class labels refer to a building pixel in the existing data base found also to be a building pixel at the later epoch. Similarly, *demolished* building and *demolished building part* have the same interpretation for a single pixel, as have *new* building and *new building part*. On a per-pixel level, it makes sense to merge these pairs of classes, forming the new classes *confirmed building pixel*, *new building pixel*, and *demolished building pixel*. The confusion matrix and the quality metrics for these classes are shown in Table 3. The quality metrics are better than those in Table 2. For *confirmed building pixels*, both completeness and correctness are larger than 95%. Completeness is reasonably good for all classes. Only for *new building pixels* it is slightly below 90%, which is caused by problems at the outlines of buildings that are very close to each other. The major error sources are a relative large number of *new building pixels* corresponding to the background in the reference and the large number of false positive *demolished building pixels* corresponding to the small buildings in the backyards that were not detected by the algorithm.

	Cf (A)	*Cd (A)*	*N_P (A)*	*N (A)*	*D_P (A)*	*D (A)*	*B (A)*
Cf (R)	50440	6190	0	0	1033	5822	4
Cd (R)	7257	77243	0	0	88	0	0
N_P (R)	0	0	4340	2362	0	0	128
N (R)	0	1261	1719	9510	0	0	621
D_P (R)	0	785	0	0	6040	0	0
D (R)	0	0	0	0	0	15664	0
B (R)	0	0	1702	2128	0	0	593163

Table 1. Confusion matrix for Fairfield [pixels]. *A*: Automatic, *R*: Reference. *Cf*: *confirmed*, *Cd*: *changed*, *N_P*: *new building part*, *N*: *new* building, *D_P*: *demolished building part*, *D*: *demolished* building, *B*: *Background*.

	Cf	*Cd*	*N_P*	*N*	*D_P*	*D*	*B*
Completeness [%]	79.4	91.3	63.5	72.5	88.5	100.0	99.4
Correctness [%]	87.4	90.4	55.9	67.9	84.3	72.9	99.9

Table 2. Completeness and correctness for Fairfield, derived from the confusion matrix in Table 1.

	C (A)	*N (A)*	*D (A)*	*B (A)*	*Comp [%]*
C (R)	141130	0	6943	4	95.3
N (R)	1261	17931	0	749	89.9
D (R)	785	0	21704	0	96.5
B (R)	0	3830	0	593163	99.4
Corr [%]	98.6	82.4	75.8	99.9	

Table 3. Confusion matrix [pixels] and completeness (*Comp*) and correctness (*Corr*) for Fairfield, using a reduced set of classes. *A*: Automatic, *R*: Reference. *C*: *confirmed pixel*, *N*: *new building pixel*, *D*: *demolished building pixel*, *B*: *Background*.

The ultimate outcome of automatic change detection is an updated version of the data base. From that point of view, only the classes *building* and *no building* are to be discerned. The resulting values of completeness and correctness for building pixels are 95.4% and 97.2%, respectively. These excellent quality metrics are relevant if the change detection results are used directly to generate the new content of the data base.

In a semi-automatic work flow as described in Section 1, per-building quality metrics are more closely linked to the effectiveness of the automated procedure. Table 4 presents the completeness and the correctness of the change detection results on a per-building basis. There are two major error sources: a relatively large number of *confirmed* buildings classified as *changed* (13), and a large number of buildings classified as *demolished* despite not having changed at all (48). This results in a very low completeness for *confirmed* buildings, and in a very low *correctness* for *changed* and *demolished* buildings. If the results of automatic change detection are used in a semi-automatic context to highlight areas of change, the number of correctly detected *confirmed* buildings is related to the amount of work that is saved by the process because *confirmed* buildings need no further inspection. However, the classification of *confirmed* buildings should be reliable in order not to save work at the expense of missed changes. There is only one false positive *confirmed* building. It is building *a* in Fig. 2, where a *new building part* was erroneously classified as a *new* building. The user would inspect the actual change (the *new* building) anyway, so that no error would be committed by not checking that building. Thus, the assumption that buildings classified as *confirmed* need no further inspection is justified. The numbers in Table 4 are affected by the poor separability of *new buildings* and *new building parts*: two of the three false negative and one of five false positive *new* buildings can be attributed to this problem. If change detection were carried out manually, the user would have to inspect all buildings in the existing data base (184) and detect the new ones (17). Of the existing buildings, 78 or 42.4% need no further attention. This is a considerable reduction of the work load of a human operator. In addition, new buildings are highlighted, with only one "real" false negative.

	Cf	*Cd*	*D*	*N*
Completeness [%]	56.1	88.9	100.0	84.2
Correctness [%]	98.7	51.6	20.0	76.2

Table 4. Completeness and correctness for Fairfield on a per-building basis. *Cf*: *confirmed building*, *Cd*: *changed building*, *N*: *new building*, *D*: *demolished building*.

The effectiveness of the automatic change detection module is restricted by the large number of missed small buildings. In (Rottensteiner, 2007), it was shown that buildings smaller than 50 m^2 could hardly be detected using ALS data of 1 m resolution. In many building data bases, such small buildings are not considered. If this is the case, the effectiveness of automatic change detection is much higher, because the changes affecting larger buildings are reliably detected. Table 5 presents completeness and correctness for buildings having an area larger than 50 m^2. There is a considerable improvement in the quality numbers. The number of existing buildings requiring inspection is 109, of which 65 or 59.6% are correctly classified as *confirmed*. Again, the quality metrics are affected by the problems related to the separability of classes. For instance, the remaining *new* buildings missed by the algorithm are classified as *new building parts* of a *changed* building, so that actually all *new* buildings were highlighted by the algorithm.

3.3.2 Toulouse: Table 6 shows completeness and correctness on a per-pixel basis for the classes distinguished by the change detection algorithm for Toulouse. These numbers are affected by the same problems of separability as those for Fairfield (cf. Table 2), but they are considerably worse because the building detection algorithm requires a high-quality DSM. For instance, as most of the pixels in the two large areas of false positive

building pixels highlighted in Fig. 3 are classified as *new building part*, the correctness of that class is only 2.7%.

Table 7 presents completeness and correctness for a restricted number of classes generated by merging the classes having a similar interpretation on a per-pixel level. The numbers are better than those in Table 6, but still not as good as those achieved in Fairfield. The correctness of *new building pixels* remains low. If only the classes *building* and *no building* are discerned, completeness and correctness are 86.9% and 71.0%, respectively. Due to errors at the building outlines, correctness is only improved to 76.9% if the two areas of false positives in Fig. 3 are eliminated. Although a visual inspection of Fig. 3 seems to indicate that some changes have been detected correctly, the quality of the DSM is not good enough for the algorithm to work effectively. This is emphasised by the fact that only one building is found to be *confirmed*; thus, only one building need not be inspected in a semi-automated work flow.

	Cf	*Cd*	*D*	*N*
Completeness [%]	81.3	88.9	100.0	88.9
Correctness [%]	98.5	55.2	75.0	76.2

Table 5. Completeness and correctness on a per-building basis for buildings larger than 50 m^2 in Fairfield. *Cf*: *confirmed building*, *Cd*: *changed building*, *N*: *new building*, *D*: *demolished building*.

	Cf	*Cd*	*S*	N_P	*N*	D_P	*D*	*B*
Comp [%]	10.2	74.8	100.0	47.4	67.5	72.9	68.8	97.0
Corr [%]	84.1	75.1	12.9	2.7	52.4	53.6	60.4	99.7

Table 6. Completeness (*Comp*) and correctness (*Corr*) on a per-pixel basis for Toulouse. *Cf*: *confirmed*, *Cd*: *changed*, *S*: *split off*, N_P: *new building part*, *N*: *new building*, D_P: *demolished building part*, *D*: *demolished building*, *B*: *Background*.

	C	*N*	*D*	*B*
Completeness [%]	81.2	71.1	80.7	97.0
Correctness [%]	95.1	17.2	63.1	99.7

Table 7. Completeness and correctness on a per-pixel basis for Toulouse, using a restricted number of classes. *C*: *confirmed pixel*, *N*: *new building pixel*, *D*: *demolished building pixel*, *B*: *Background*.

4. CONCLUSIONS

A method for change detection for updating building data bases from DSMs and an NDVI image was evaluated. The results of change detection are presented so that the user can easily assess which buildings are *confirmed*, *new*, *demolished*, or *changed*, and in case of *changed* buildings also the nature and extent of these changes. The evaluation has shown that some of these classes cannot be discerned reliably even under good circumstances. This partly due to the nature of the problem, because the appearance of a new building and an addition to an existing building might be identical in remotely sensed data. The quality of the results is also restricted by the accuracy and the resolution of the sensor data in relation to the building size: small buildings are often missed by the building detection algorithm if the DSM resolution is about 1 m. For good DSMs, good results could be achieved on a per-pixel level, with both completeness and correctness of the results being above 95%. Thus, if the remaining problems with small buildings and with building outlines are negligible for the data base to be updated, the change detection algorithm can be used to automatically derive the new state of the data base. If the accuracy requirements are very high, the change detection process can be embedded in a semi-automatic working environment to highlight areas of change to a human operator. It was shown that such an approach can reduce the amount of human intervention by 40% even in the presence of many small buildings. If only buildings larger than 50 m^2 are considered, the reduction was almost 60%. It is one restriction of the algorithm that it requires an excellent DSM. Good results can be expected for ALS-based DSMs having a resolution of 1 m or better. In our experiments, the results achieved using a DSM generated by image matching were not very good, because the DSM quality was not sufficient for the algorithm. This may be due to problems of the specific matching algorithm used to generate the Toulouse DSM, and our findings thus cannot be generalized for all DSMs generated from imagery. Applying advanced image matching techniques and/or multiple-overlap imagery might alleviate the problems found with the Toulouse DSMs. Future work will concentrate on improving the geometrical quality of the building outlines by image edges.

ACKNOWLEDGEMENTS

The Fairfield data set was provided by AAMHatch, Australia (www.aamhatch.com.au). The Toulouse data set was distributed by EuroSDR in their test on the detection of unregistered buildings for updating cadastral data bases (EuroSDR, 2007).

REFERENCES

Champion, N., 2007. 2D Building change detection from high resolution aerial images and correlation digital surface models. In: *IAPRSIS* XXXVI-3 / W49A, pp. 197-202.

EuroSDR, 2007. Detection of unregistered buildings for updating cadastral databases. http://buildingsdetection.free.fr (accessed 19 Nov. 2007).

Matikainen, L., Hyyppä, J., Kaartinen, H., 2004. Automatic detection of changes from laser scanner and aerial image data for updating building maps. In: *IAPRSIS* XXXV-B2, pp. 434-439.

Rottensteiner, F., Trinder, J., Clode, S., Kubik, K., 2007. Building detection by fusion of airborne laserscanner data and multi-spectral images: Performance evaluation and sensitivity analysis. *ISPRS Journal for Photogrammetry and Remote Sensing*, 62(2), pp. 135–149.

Rottensteiner, F., 2007. Building change detection from digital surface models and multi-spectral images. In: *IAPRSIS* XXXVI-3 / W49B (on CD-ROM).

Vögtle, T., Steinle, E., 2004. Detection and recognition of changes in building geometry derived from multitemporal laserscanning data. In: *IAPRSIS* XXXV-B2, pp. 428-433.

Vosselman, G., Gorte, B., Sithole, G., 2004. Change detection for updating medium scale maps using laser altimetry. In: *IAPRSIS* XXXV-B3, pp. 207-212.